AIP Applied Physics Letters

Conduction band energies and hot-electron transport characteristics of epitaxial Sc 2 O 3/Si (111) studied by ballistic electron emission microscopy and internal photoemission

W. Cai, S. E. Stone, J. P. Pelz, L. F. Edge, and D. G. Schlom

Citation: Applied Physics Letters **91**, 042901 (2007); doi: 10.1063/1.2757150
View online: http://dx.doi.org/10.1063/1.2757150
View Table of Contents: http://scitation.aip.org/content/aip/journal/apl/91/4?ver=pdfcov
Published by the AIP Publishing

Articles you may be interested in
Hot-electron transport studies of the Ag/Si(001) interface using ballistic electron emission microscopy
J. Vac. Sci. Technol. A **28**, 643 (2010); 10.1116/1.3397795

Avalanche ballistic electron emission microscopy with single hot-electron sensitivity
Appl. Phys. Lett. **83**, 2841 (2003); 10.1063/1.1613996

Energy-dependent conduction band mass of SiO 2 determined by ballistic electron emission microscopy
J. Vac. Sci. Technol. B **17**, 1823 (1999); 10.1116/1.590833

Hot-electron transport through Au/CaF 2 /Si (111) structure studied by ballistic electron emission spectroscopy
J. Appl. Phys. **85**, 941 (1999); 10.1063/1.369214

Ballistic electron emission microscopy study of Schottky contacts on 6H- and 4H- SiC
Appl. Phys. Lett. **72**, 839 (1998); 10.1063/1.120910

This article is copyrighted as indicated in the article. Reuse of AIP content is subject to the terms at: http://scitation.aip.org/termsconditions. Downloaded to IP: 128.84.143.26 On: Mon, 11 May 2015 13:50:01

Conduction band energies and hot-electron transport characteristics of epitaxial Sc_2O_3/Si (111) studied by ballistic electron emission microscopy and internal photoemission

W. Cai,[a)] S. E. Stone, and J. P. Pelz[b)]
Department of Physics, The Ohio State University, Columbus, Ohio 43210

L. F. Edge and D. G. Schlom
Department of Materials Science and Engineering, Pennsylvania State University, University Park, Pennsylvania 16802-5005

(Received 26 April 2007; accepted 19 June 2007; published online 24 July 2007)

Ballistic electron emission microscopy (BEEM) and internal photoemission measurements on a 20-nm-thick epitaxial Sc_2O_3 film on Si (111) show the existence of a lower "tail state" conduction band (CB) extending ~0.9 eV below the upper CB (similar to that reported for amorphous Sc_2O_3 films), indicating that these states are not simply due to disorder in amorphous films. This lower CB is also found to support elastic hot-electron transport even against an applied electric field, indicating transport via extended rather than localized states. © *2007 American Institute of Physics*.
[DOI: 10.1063/1.2757150]

The continued scaling of Si-based metal-oxide-semiconductor electronics raises interest in replacing SiO_2 with a "high-*k*" (higher dielectric constant) material.[1] A thicker high-*k* film has the same capacitance as a (thinner) SiO_2 film but with reduced direct tunnel current, provided the energy barriers for electron and hole tunneling remain sufficiently large. This makes it critical to understand the band structure of potential high-*k* materials, and in particular the conduction and valence band offsets to Si. Recently, photoconductivity (PC) and internal photoemission (Int-PE) measurements have been used to investigate the band gaps and band offsets to Si of a number of potential high-*k* amorphous metal oxide films[2–8] (including amorphous HfO_2, Sc_2O_3, $LaAlO_3$, $GdScO_3$, $DyScO_3$, $LaScO_3$, Lu_2O_3, and $La_2Hf_2O_7$). Surprisingly, most of these amorphous films were found to have nearly the same band gap (~5.6–5.8 eV), conduction band (CB) offset (~2.0–2.1 eV), and valence band (VB) offset (~2.4–2.6 eV). Furthermore, many of these films have a secondary conduction band (sometimes referred to as a "tail state" band) extending ~1 eV below the assumed primary CB, with possible physical origin attributed to disorder in the amorphous oxide film[2,5] or the different symmetries or *d*-state coupling in complex oxides with mixed metal cations.[6]

Here, we report measurements using ballistic electron emission microscopy (BEEM) (Refs. 9–12) in combination with Int-PE and PC to investigate band alignment and carrier transport in a 20-nm-thick crystalline Sc_2O_3 film grown epitaxially at 700 °C on a Si(111) substrate using both Pt and Al metal contacts. Int-PE measurements from the Si side of the epi-Sc_2O_3 film show an ~1.9 eV Sc_2O_3/Si CB offset, similar to the recently reported[7] ~2.0 eV CB offset for amorphous Sc_2O_3, and also a lower CB extending ~0.9 eV below the main CB, similar reports for amorphous Sc_2O_3 (Ref. 7) and a variety of other amorphous oxide films.[6,7] This indicates that these tail states are not simply due to disorder in the amorphous films. PC measurements of the epi-Sc_2O_3 film also show the same ~6.0 eV band gap as seen on crystallized Sc_2O_3.[13,14] Both BEEM and Int-PE from the metal side show strong electron transport through the lower CB. Most significantly the BEEM data clearly show that this lower CB supports *elastic* transport across the 20-nm-thick epi-Sc_2O_3 even against an applied electric field, and so is a robust CB consisting of *extended* rather than localized states.

The 20-nm-thick epitaxial Sc_2O_3 film was grown at 700 °C on a *p*+ (0.02–0.06 Ω cm) boron-doped Si(111) substrate by reactive molecular-beam epitaxy[15] at a background pressure of molecular oxygen of 2×10^{-6} Torr, which is 100 times greater than that needed to fully oxidize the incident scandium metal flux at room temperature. Before growth, the bare Si(111) substrate was wet cleaned in dilute hydrofluoric acid to hydrogen terminate its surface before loading into the MBE chamber. It was heated in ultrahigh vacuum (UHV) to 700 °C for the growth of Sc_2O_3. Four-circle x-ray diffraction indicated that the Sc_2O_3 film was epitaxial with (111) $Sc_2O_3\|(111)$Si and mixed *A*-type and *B*-type alignments to the underlying Si(111),[16] i.e., the epitaxial films contain two twin variants related by a 180° in-plane rotation. The full width at half maximum of the rocking curve of the 222 Sc_2O_3 reflection was 0.064°.

After exposure to air the Sc_2O_3/Si samples were degreased using organic solvents, rinsed in de-ionized water, and coated with AZ5214E photoresist. Photolithography was used to open a number of 45 μm square "windows" as well as a large clear region on one side of the sample. After a 30 min bake at 170 °C and a brief UV-ozone clean (to removed photoresist residue over the open regions) the samples were immediately introduced into an UHV preparation chamber, and heated to ~250–340 °C for 10 min to desorb water and hydrocarbons. ~5 nm thick Pt or Al films were then deposited by electron beam evaporation through a shadow mask to form a number of 0.5 mm diameter "dots." The samples were then transported *in situ* to an adjacent UHV for BEEM and Int-PE measurements. Metal dots over the 45 μm windows were used for the BEEM measurements

[a)]Electronic mail: cai.54@osu.edu
[b)]Electronic mail: pelz.2@osu.edu

This article is copyrighted as indicated in the article. Reuse of AIP content is subject to the terms at: http://scitation.aip.org/termsconditions. Downloaded to IP: 128.84.143.26 On: Mon, 11 May 2015 13:50:01
 © 2007 American Institute of Physics

(to reduce the metal/Sc_2O_3 contact area and hence leakage current), while metal dots over the large open area were used for Int-PE (to maximize the signal).

The BEEM measurements were done with a custom-built UHV scanning tunneling microscopy (STM)/BEEM system,[10] modified with a fiber-optic feedthrough to permit *in situ* Int-PE with photons up to ~6 eV energy, provided by a xenon lamp and a $\frac{1}{4}$ meter monochrometer. An Au wire was used to contact the metal dots.

BEEM and Int-PE measurements of dielectric films are based on similar physics in that they induce "hot" carriers with known energy distribution in a metal or semiconductor close to the dielectric film, and measure internal energy barrier heights (BHs) by determining the minimum "threshold" carrier energy required to enter and conduct across the dielectric CB or VB. Int-PE uses monochromatic photon illumination to create hot electron-hole pairs (with the BH given by the threshold photon energy E_{th}),[4] while BEEM injects either hot electrons or hot holes using the biased tip of an STM.[9–11] For sufficient photon energy, hot electron-hole pairs are also created within the dielectric and also produce a current, which is designated as PC. Since the measured Int-PE current is the *sum* of all of these processes, it is common to enhance the current from particular processes by applying a large metal bias V_{gate} to create a large "forward" ("reverse") electric field E_{ox} that pushes electrons toward the substrate (metal). The intrinsic BHs are determined by extrapolating measured BHs to zero E_{ox}.[4]

In contrast to Int-PE, BEEM injects either hot electrons or hot holes (depending on tip bias) *only* from the metal side. Hence hot carrier injection and transport *from the metal side* can be studied not only with forward E_{ox} but also with zero or reverse E_{ox}, provided the inelastic scattering length in the dielectric is sufficiently long. This permits studies of both interfaces, scattering within the dielectric, and measurements of bulk dielectric charge.[10,11]

BEEM and Int-PE spectra for the Pt/epi-Sc_2O_3/Si samples are shown in Fig. 1. The sign of the measured Int-PE current from the Si substrate switched from negative for $V_{gate} < \sim 1$ V to positive for $V_{gate} > \sim 1$ V, indicating that $E_{ox} \cong 0$ at $V_{gate} \cong 1$ V. The BEEM current measured with negative tip voltage (i.e., electrons injected into the metal) was found to be negative for all V_{gate}. No BEEM current was observed for positive tip voltage (injected holes). The V_{th} for each BEEM spectrum was determined by fitting the Bell-Kaiser model[9] for a 0.5 V range of data self-consistently centered around the best-fit value of V_{th}, as shown in Fig. 1(a). The Int-PE spectra were fitted in the conventional way[4] using a linear fit of a selected 0.2 eV range of above-threshold electron quantum yield Y data raised to the $\frac{1}{2}$ power for negative gate bias or to the $\frac{1}{3}$ power for positive gate bias[4] [see Fig. 1(b)] and extrapolating to zero yield. In the case of multiple thresholds [e.g., Fig. 1(b)] current with a lower threshold was first subtracted.[7] We estimate a statistical uncertainty of ~30 meV for the extracted BEEM and Int-PE BHs, and a systematic uncertainty of ~40 and ~80 meV, respectively. Systematic errors were estimated by varying the fitting range (while maintaining a good fit) to determine the effect on the best-fit threshold energy.

The BHs for the samples with Pt gate electrodes are summarized in Fig. 2(a). Two distinct thresholds were observed in the Int-PE spectra for $V_{gate} > 1$ V (reverse E_{ox}) at nearly the same energies as previously reported for amorphous Sc_2O_3.[7] These were identified[7] as electron injection from the Si substrate into the regular Sc_2O_3 CB (upper threshold) at ~3.0 eV above the Si VB, and a lower CB at ~2.1 eV above the Si VB. On our epitaxial samples these threshold energies were found to be almost the same when (lower work function) Al contacts were used instead of Pt, indicating that they are indeed due to electron injection at the Sc_2O_3/Si interface. Existence of this lower threshold in epitaxial Sc_2O_3 indicates the lower CB is not simply due to disorder in the amorphous film.

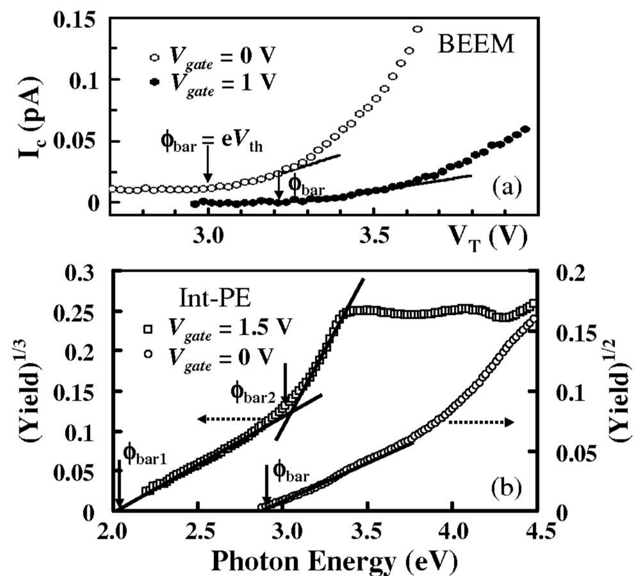

FIG. 1. (a) Typical BEEM I_c-V_T data (circles) and Bell-Kaiser model fits (solid lines) and best-fit barrier heights (arrows) for two different values of V_{gate}. Each of the data is an average of 45–49 individual I_c-V_T curves measured at different locations. Curves have been vertically offset for clarity. Tip current was 10–15 nA. (b) Int-PE yield $Y^{1/3}$ (left axis) and $Y^{1/2}$ (right axis) data (open symbols) and linear fits (solid lines) vs photon energy extrapolated to zero yield to determine barrier heights at the oxide/Si (left curve) and metal/oxide (right curve), respectively.

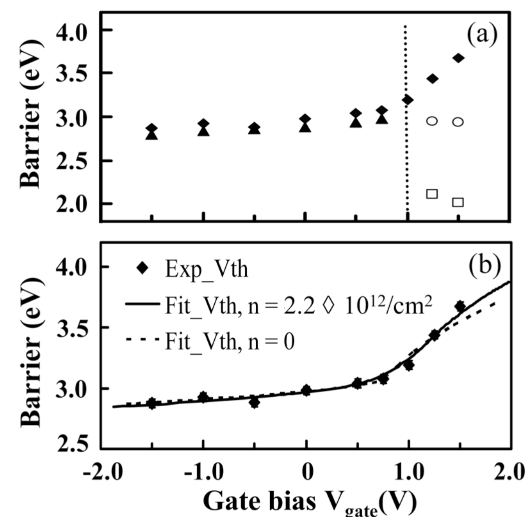

FIG. 2. (a) Best-fit barrier heights vs V_{gate} determined by BEEM (solid diamonds) and Int-PE (solid triangles and open symbols). The vertical dashed line separates conditions with forward and reverse E_{ox}. Under reverse E_{ox}, Int-PE measures two distinct barriers at the oxide/Si interface. (b) BEEM data (symbols) and model fits assuming zero oxide charge (dashed line) and $n_{bulk} = 2.2 \times 10^{12}/cm^2$ (solid line).

This article is copyrighted as indicated in the article. Reuse of AIP content is subject to the terms at: http://scitation.aip.org/termsconditions. Downloaded to IP: 128.84.143.26 On: Mon, 11 May 2015 13:50:01

For $V_{gate} < 1$ V (forward E_{ox}) Fig. 2(a) shows that the BHs measured by BEEM and Int-PE both had nearly the same energy (with systematic ~80 meV offset) and nearly the same weak dependence on V_{gate}. These BHs were substantially reduced when Al was used instead of Pt, indicating that both BEEM and Int-PE measured the same electron energy barrier at the metal/Sc_2O_3 interface. The weak dependence on V_{gate} is consistent with the "image-force lowering" effect[17] expected at the metal/Sc_2O_3 interface, and the small offset is probably due to differences in the fitting models and energy ranges used for the BEEM and Int-PE data. *In situ* premetallization sample outgassing $\geq \sim 250$ °C (as discussed earlier) was necessary to observe electron injection from the metal side, using either BEEM or Int-PE, suggesting that adsorbates at the metal/Sc_2O_3 interface can prevent electron injection from the metal.

For $V_{gate} \geq 1$ V, Fig. 2(a) shows that the BHs measured by BEEM have a sharp transition to a much stronger dependence on V_{gate}, with an approximate slope given by $dE_{bar}/d(eV_{gate}) \cong 1$. This behavior has been observed in prior BEEM measurements of metal/SiO_2/Si structures.[11,12] With the transition from forward E_{ox} to reverse E_{ox}, the high point in the CB profile abruptly switches from the (front) metal/oxide interface to the (back) oxide/Si interface, with a subsequent strong direct dependence of the BH on V_{gate}. One immediate conclusion is that at least some of the hot electrons injected into the Sc_2O_3 CB from the metal must have a long inelastic mean free path, since they can transport across the 20-nm-thick Sc_2O_3 film *even against an electric field*. We return to this point below.

Since BEEM can measure the BH continuously from forward E_{ox} to reverse E_{ox}, we should be able to determine *which* of the two CBs measured by Int-PE at the Si interface (with reverse E_{ox}) corresponds to the CB measured by Int-PE and BEEM at the metal interface (with forward E_{ox}). Figure 2(b) compares the BEEM data to model fits, which calculate how the barrier (i.e., the high-energy point in the Sc_2O_3 CB profile) varies with V_{gate}. Known parameters are the Si electron affinity $\chi_{Si}=4.05$ eV, the Si doping ($\sim 1 \times 10^{18}/cm^3$, *p* type), and the Sc_2O_3 high-frequency dielectric constant $\varepsilon_{high}=3.57$, which is necessary to calculate image force lowering at the metal interface.[17] The adjustable parameters in the fits are the metal work function (W_{Pt}), electron affinity of Sc_2O_3 (χ_{ox}), and possible negative bulk charge density in the oxide Sc_2O_3 (n_{bulk}). The dashed line in Fig. 2(b) shows the fit assuming $n_{bulk}=0$, with best fit values $W_{Pt}=5.88$ eV and $\chi_{ox}=2.79$ eV, while the solid line shows the fit with n_{bulk} as a free parameter, with $W_{Pt}=5.97$ eV and $\chi_{ox}=2.91$ eV, and $n_{bulk}=2.2 \times 10^{12}$ cm^{-2} (projected areal electron density). The solid line in Fig. 3 shows the corresponding calculated CB profile (with $n_{bulk}=2.2 \times 10^{12}$ cm^{-2}) at an ~1.5 V gate bias.

For comparison, the two dashed lines in Fig. 3 represent the upper and lower CBs as determined by Int-PE from the Si side. We see that the CB measured by BEEM and Int-PE from the metal side most closely lines up with the *lower* CB measured by Int-PE from the Si side. This indicates that the lower band extends all the way through the 20 nm thick Sc_2O_3 film and is not localized only at the Sc_2O_3/Si interface. Furthermore, Fig. 2 shows that BEEM is able to inject hot electrons completely across the Sc_2O_3 film up to $V_{gate}=+1.5$ V, where the electrons must move *against* an electric field in the Sc_2O_3 film. This indicates that the inelastic mean-free path in this CB must be a sizeable fraction of the 20 nm film thickness. Consequently, electron conduction in this CB cannot consist only of thermally activated electron hopping as one might expect of a band of localized "tail states."

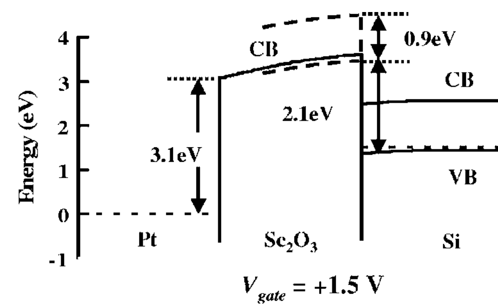

FIG. 3. Solid line is the energy band diagram of Pt/Sc_2O_3/Si for $V_{gate}=+1.5$ V determined from the solid-line model fit to the BEEM data in Fig. 2(b). The dashed lines show the energies of the two CB minima at the oxide/Si interface determined by Int-PE with reverse E_{ox}. At the oxide/Si interface, the CB determined by BEEM best matches the lower of the two CBs determined by Int-PE. The curvature of the conduction band of Sc_2O_3 is caused by the fixed charge in the oxide.

In summary, BEEM and Int-PE measurements on 20-nm-thick epitaxial Sc_2O_3/Si (111) films show the existence of a lower conduction band extending ~0.9 eV below the main CB, as have been reported for a variety of amorphous oxide films,[6,7] indicating that these states are not simply due to disorder in the amorphous films. This lower CB supports *ballistic* hot-electron transport across the epi-Sc_2O_3 even against an applied electric field, indicating that it consists of *extended* rather than localized states.

This work was supported by the Semiconductor Research Corp. and by the National Science Foundation Grant No. DMR-0505165. One of the authors (L.F.E.) gratefully acknowledges the AMD/SRC fellowship.

[1]International Technology Roadmap for Semiconductors, 2005 ed. (http://www.itrs.net/Links/2005ITRS/Home2005.htm), pp. 2 and 22–36.
[2]V. V. Afanas'ev, M. Houssa, A. Stesmans, and M. M. Heyns, Appl. Phys. Lett. **78**, 3073 (2001).
[3]V. V. Afanas'ev, A. Stesmans, F. Chen, X. Shi, and S. A. Campbell, Appl. Phys. Lett. **81**, 1053 (2002).
[4]V. V. Afanas'ev, M. Houssa, A. Stesmans, and M. M. Heyns, J. Appl. Phys. **91**, 3079 (2002).
[5]G. Seguini, E. Bonera, S. Spiga, G. Scarel, and M. Fanciulli, Appl. Phys. Lett. **85**, 5316 (2004).
[6]V. V. Afanas'ev, A. Stesmans, C. Zhao, M. Caymax, T. Heeg, J. Schubert, Y. Jia, D. G. Schlom, and G. Lucovsky, Appl. Phys. Lett. **85**, 5917 (2004).
[7]V. V. Afanas'ev, A. Stesmans, L. F. Edge, D. G. Schlom, T. Heeg, and J. Schubert, Appl. Phys. Lett. **88**, 032104 (2006).
[8]G. Seguini, S. Spiga, E. Bonera, M. Fanciulli, A. Reyes Huamantinco, C. J. Först, C. R. Ashman, P. E. Blöchl, A. Dimoulas, and G. Mavrou, Appl. Phys. Lett. **88**, 202903 (2006).
[9]W. J. Kaiser and L. D. Bell, Phys. Rev. Lett. **60**, 1406 (1988); **61**, 2368 (1988).
[10]B. Kaczer, Z. Meng, and J. P. Pelz, Phys. Rev. Lett. **77**, 91 (1996).
[11]B. Kaczer, H.-J. Im, J. P. Pelz, and R. M. Wallace, Appl. Phys. Lett. **73**, 1871 (1998).
[12]R. Ludeke, A. Bauer, and E. Cartier, Appl. Phys. Lett. **66**, 730 (1995).
[13]H. H. Tippins, J. Phys. Chem. Solids **27**, 1069 (1966).
[14]V. N. Abramov, A. N. Ermoshkin, and A. I. Kuznetsov, Sov. Phys. Solid State **25**, 981 (1983).
[15]D. O. Klenov, L. F. Edge, D. G. Schlom, and S. Stemmer, Appl. Phys. Lett. **86**, 051901 (2005).
[16]R. T. Tung, J. C. Bean, J. M. Gibson, J. M. Poate, and D. C. Jacobson, Appl. Phys. Lett. **40**, 684 (1982).
[17]S. M. Sze, *Physics of Semiconductor Devices* (Wiley, New York, 1981), 2nd ed., pp. 250–254.

This article is copyrighted as indicated in the article. Reuse of AIP content is subject to the terms at: http://scitation.aip.org/termsconditions. Downloaded to IP: 128.84.143.26 On: Mon, 11 May 2015 13:50:01